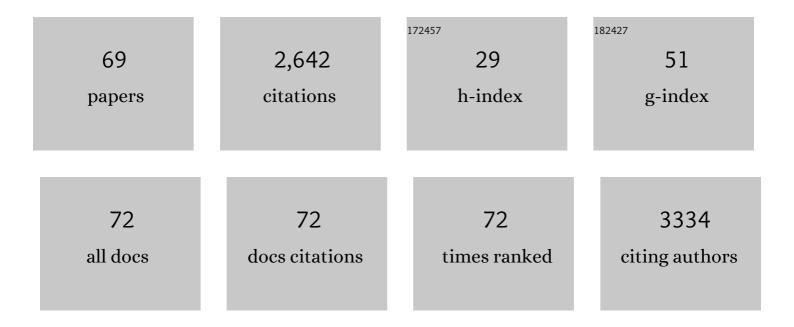
Lisa A Delouise

List of Publications by Year in descending order

Source: https://exaly.com/author-pdf/2107255/publications.pdf Version: 2024-02-01



#	Article	IF	CITATIONS
1	Encapsulation of Primary Salivary Gland Acinar Cell Clusters and Intercalated Ducts (AIDUCs) within Matrix Metalloproteinase (MMP)â€Degradable Hydrogels to Maintain Tissue Structure and Function. Advanced Healthcare Materials, 2022, 11, e2101948.	7.6	7
2	Optimizing Soluble Cues for Salivary Cland Tissue Mimetics Using a Design of Experiments (DoE) Approach. Cells, 2022, 11, 1962.	4.1	2
3	Development of a functional salivary gland tissue chip with potential for high-content drug screening. Communications Biology, 2021, 4, 361.	4.4	30
4	Salivary Gland Tissue Engineering Approaches: State of the Art and Future Directions. Cells, 2021, 10, 1723.	4.1	13
5	The UVR Filter Octinoxate Modulates Aryl Hydrocarbon Receptor Signaling in Keratinocytes via Inhibition of CYP1A1 and CYP1B1. Toxicological Sciences, 2020, 177, 188-201.	3.1	0
6	Silicon Nanomembrane Filtration and Imaging for the Evaluation of Microplastic Entrainment along a Municipal Water Delivery Route. Sustainability, 2020, 12, 10655.	3.2	1
7	Morphology-Dependent Titanium Dioxide Nanoparticle-Induced Keratinocyte Toxicity And Exacerbation Of Allergic Contact Dermatitis. Toxicology Current Research, 2020, 4, 1-7.	0.2	3
8	Further studies in translatable model systems are needed to predict the impacts of human microplastic exposure. Open Access Journal of Toxicology, 2020, 4, 79-82.	0.3	0
9	Microsystems technology for high-throughput single-cell sorting. , 2019, , 701-719.		0
10	Amorphous silicon dioxide nanoparticles modulate immune responses in a model of allergic contact dermatitis. Scientific Reports, 2019, 9, 5085.	3.3	16
11	Multi-walled carbon nanotube oxidation dependent keratinocyte cytotoxicity and skin inflammation. Particle and Fibre Toxicology, 2019, 16, 3.	6.2	37
12	From Dose to Response: In Vivo Nanoparticle Processing and Potential Toxicity. Advances in Experimental Medicine and Biology, 2017, 947, 71-100.	1.6	41
13	Identifying drug resistant cancer cells using microbubble well arrays. Biomedical Microdevices, 2017, 19, 17.	2.8	3
14	Effect of Nanoparticle Surface Coating on Cell Toxicity and Mitochondria Uptake. Journal of Biomedical Nanotechnology, 2017, 13, 155-166.	1.1	35
15	Immunomodulatory Effects of Nanoparticles on Skin Allergy. Scientific Reports, 2017, 7, 3979.	3.3	30
16	In vivo quantification of quantum dot systemic transport in C57BL/6 hairless mice following skin application post-ultraviolet radiation. Particle and Fibre Toxicology, 2017, 14, 12.	6.2	12
17	Impact of Cosmetic Lotions on Nanoparticle Penetration through ex Vivo C57BL/6 Hairless Mouse and Human Skin: A Comparison Study. Cosmetics, 2016, 3, 6.	3.3	34
18	Nanoparticle-Enabled Transdermal Drug Delivery Systems for Enhanced Dose Control and Tissue Targeting. Molecules, 2016, 21, 1719.	3.8	178

LISA A DELOUISE

#	Article	IF	CITATIONS
19	In vitro assays for determining the metastatic potential of melanoma cell lines with characterized in vivo invasiveness. Biomedical Microdevices, 2016, 18, 89.	2.8	9
20	UVB Dependence of Quantum Dot Reactive Oxygen Species Generation in Common Skin Cell Models. Journal of Biomedical Nanotechnology, 2015, 11, 1644-1652.	1.1	8
21	Development and characterization of antibody reagents for detecting nanoparticles. Nanoscale, 2015, 7, 20042-20054.	5.6	3
22	Quantitative analysis of spherical microbubble cavity array formation in thermally cured polydimethylsiloxane for use in cell sorting applications. Biomedical Microdevices, 2014, 16, 55-67.	2.8	12
23	Understanding engineered nanomaterial skin interactions and the modulatory effects of ultraviolet radiation skin exposure. Wiley Interdisciplinary Reviews: Nanomedicine and Nanobiotechnology, 2014, 6, 61-79.	6.1	35
24	Microbubble array diffusion assay for the detection of cell secreted factors. Lab on A Chip, 2014, 14, 3640-3650.	6.0	9
25	The impact of UVB exposure and differentiation state of primary keratinocytes on their interaction with quantum dots. Nanotoxicology, 2013, 7, 1244-1254.	3.0	7
26	Characterization of cell seeding and specific capture of B cells in microbubble well arrays. Biomedical Microdevices, 2013, 15, 453-463.	2.8	10
27	Thiol Antioxidant-Functionalized CdSe/ZnS Quantum Dots: Synthesis, Characterization, Cytotoxicity. Journal of Biomedical Nanotechnology, 2013, 9, 382-392.	1.1	28
28	Quantification of quantum dot murine skin penetration with UVR barrier impairment. Nanotoxicology, 2013, 7, 1386-1398.	3.0	27
29	Applications of Nanotechnology in Dermatology. Journal of Investigative Dermatology, 2012, 132, 964-975.	0.7	155
30	Effect of homotypic and heterotypic interaction in 3D on the E-selectin mediated adhesive properties of breast cancer cell lines. Biomaterials, 2012, 33, 9037-9048.	11.4	35
31	Quantification of human skin barrier function and susceptibility to quantum dot skin penetration. Nanotoxicology, 2011, 5, 675-686.	3.0	22
32	Near-IR fluorescence and reflectance confocal microscopy for imaging of quantum dots in mammalian skin. Biomedical Optics Express, 2011, 2, 1610.	2.9	14
33	Continuously perfused microbubble array for 3D tumor spheroid model. Biomicrofluidics, 2011, 5, 24110.	2.4	72
34	The Cytotoxicity of OPA-Modified CdSe/ZnS Core/Shell Quantum Dots and Its Modulation by Silibinin in Human Skin Cells. Journal of Biomedical Nanotechnology, 2011, 7, 648-658.	1.1	9
35	Microenvironment induced spheroid to sheeting transition of immortalized human keratinocytes (HaCaT) cultured in microbubbles formed in polydimethylsiloxane. Biomaterials, 2011, 32, 7159-7168.	11.4	30
36	Enriching and characterizing cancer stem cell sub-populations in the WM115 melanoma cell line. Biomaterials, 2011, 32, 9316-9327.	11.4	30

LISA A DELOUISE

#	Article	IF	CITATIONS
37	Detection of the Cancer Marker CD146 Expression in Melanoma Cells with Semiconductor Quantum Dot Label. Journal of Biomedical Nanotechnology, 2010, 6, 303-311.	1.1	17
38	Integration of a Chemicalâ€Responsive Hydrogel into a Porous Silicon Photonic Sensor for Visual Colorimetric Readout. Advanced Functional Materials, 2010, 20, 573-578.	14.9	76
39	Tunable Detection Sensitivity of Opiates in Urine via a Label-Free Porous Silicon Competitive Inhibition Immunosensor. Analytical Chemistry, 2010, 82, 714-722.	6.5	45
40	Label-Free Porous Silicon Immunosensor for Broad Detection of Opiates in a Blind Clinical Study and Results Comparison to Commercial Analytical Chemistry Techniques. Analytical Chemistry, 2010, 82, 9711-9718.	6.5	49
41	Hybrid nanoporous silicon optical biosensor architectures for biological sample analysis. Proceedings of SPIE, 2010, , .	0.8	2
42	Progress and Challenges in Quantifying Skin Permeability to Nanoparticles Using a Quantum Dot Model. Journal of Biomedical Nanotechnology, 2010, 6, 596-604.	1.1	9
43	Increased in vivo skin penetration of quantum dots with UVR and in vitro quantum dot cytotoxicity. , 2009, , .		7
44	Reusable linking chemistry for Hisâ€6 tagged proteins in an affinityâ€based porous silicon biosensor. Physica Status Solidi (A) Applications and Materials Science, 2009, 206, 1299-1305.	1.8	2
45	Physicochemical factors that affect metal and metal oxide nanoparticle passage across epithelial barriers. Wiley Interdisciplinary Reviews: Nanomedicine and Nanobiotechnology, 2009, 1, 434-450.	6.1	66
46	Photoinduced fluorescence enhancement and energy transfer effects of quantum dots porous silicon. Physica Status Solidi C: Current Topics in Solid State Physics, 2009, 6, 1729-1735.	0.8	20
47	Design of a hybrid amine functionalized polyacrylamide hydrogel-porous silicon optical sensor. , 2009, , .		4
48	Breeching Epithelial Barriers – Physiochemical Factors Impacting Nanomaterial Translocation and Toxicity. Nanostructure Science and Technology, 2009, , 33-62.	0.1	4
49	Microfabrication of Bubbular Cavities in PDMS for Cell Sorting and Microcell Culture Applications. Journal of Bionic Engineering, 2008, 5, 308-316.	5.0	22
50	In Vivo Skin Penetration of Quantum Dot Nanoparticles in the Murine Model: The Effect of UVR. Nano Letters, 2008, 8, 2779-2787.	9.1	273
51	Label-Free Optical Detection of Peptide Synthesis on a Porous Silicon Scaffold/Sensor. Langmuir, 2008, 24, 2908-2915.	3.5	18
52	Optical Detection of Polyacrylamide Swelling Behavior in a Porous Silicon Sensor. Materials Research Society Symposia Proceedings, 2008, 1133, 1.	0.1	1
53	Enhancement of the evanescent field using polymer waveguides fabricated by deep UV exposure on mesoporous silicon. Optics Letters, 2007, 32, 2843.	3.3	12
54	Microfabrication of cavities in polydimethylsiloxane using DRIE silicon molds. Lab on A Chip, 2007, 7, 1660.	6.0	51

LISA A DELOUISE

#	Article	IF	CITATIONS
55	Steric Crowding Effects on Target Detection in an Affinity Biosensor. Langmuir, 2007, 23, 5817-5823.	3.5	92
56	Label-Free Quantitative Detection of Protein Using Macroporous Silicon Photonic Bandgap Biosensors. Analytical Chemistry, 2007, 79, 1502-1506.	6.5	97
57	Whole blood optical biosensor. Biosensors and Bioelectronics, 2007, 23, 444-448.	10.1	101
58	Hydrogel-Supported Optical-Microcavity Sensors. Advanced Materials, 2005, 17, 2199-2203.	21.0	60
59	Enzyme Immobilization in Porous Silicon:  Quantitative Analysis of the Kinetic Parameters for Glutathione-S-transferases. Analytical Chemistry, 2005, 77, 1950-1956.	6.5	97
60	Cross-Correlation of Optical Microcavity Biosensor Response with Immobilized Enzyme Activity. Insights into Biosensor Sensitivity. Analytical Chemistry, 2005, 77, 3222-3230.	6.5	131
61	Quantatitive Assessment of Enzyme Immobilization Capacity in Porous Silicon. Analytical Chemistry, 2004, 76, 6915-6920.	6.5	71
62	Surface chemistry on semiconductors studied by molecular-beam reactive scattering. Surface Science Reports, 1994, 19, 285-380.	7.2	94
63	Dynamical study of the Ar+ ion-enhanced Cl2/GaAs s(110) etch rate phenomenon. Vacuum, 1992, 43, 1083-1085.	3.5	3
64	Defect induced surface chemistry: A comparison of the adsorption and thermal decomposition of C2H4 on Rh{111} and Rh{331}. Surface Science, 1990, 230, 35-46.	1.9	24
65	The influence of surface atomic steps on site-selective adsorption processes. Ethylidyne formation on rhodium{111} and rhodium{331}. Journal of the American Chemical Society, 1987, 109, 6873-6875.	13.7	16
66	Adsorption and desorption of no from Rh{111} and Rh{331} surfaces. Surface Science, 1985, 159, 199-213.	1.9	105
67	Velocity dependence of azimuthal anisotropies in ion scattering from rhodium {111}. Surface Science, 1985, 154, 22-34.	1.9	16
68	CHaracterization of CO binding sites on Rh{111} and Rh{331} surfaces by XPS and LEED: Comparison to EELS results. Surface Science, 1984, 147, 252-262.	1.9	40
69	Carbon monoxide adsorption and desorption on Rh{111} and Rh{331} surfaces. Surface Science, 1984, 138, 417-431.	1.9	59